UNIVERSITÀ DI PARMA
ARCHIVIO DELLA RICERCA

University of Parma Research Repository

Predictive control of a combined heat and power plant for grid flexibility under demand uncertainty

note finali coverpage

(Article begins on next page)

13 January 2025

Predictive control of a combined heat and power plant for grid flexibility under demand uncertainty[1]

Andrea De Lorenzi[a], Agostino Gambarotta[a,b], Emanuela Marzi[b],
Mirko Morini[a,b], Costanza Saletti[b*]

[a] *Center for Energy and Environment (CIDEA), University of Parma, Parco Area delle Scienze 42, 43124 Parma, Italy*
[b] *Department of Engineering and Architecture, University of Parma, Parco Area delle Scienze 181/A, 43124 Parma, Italy*

** Corresponding author: costanza.saletti@unipr.it

Abstract

In recent years, the increasing penetration of non-programmable renewable energy technologies has made energy system flexibility essential for ensuring power grid stability, in terms of balance between power demand and supply. In particular, cogeneration plants can provide flexibility services by making a defined amount of power available at a given schedule, upon request. The grid operator can request it or not depending on the actual dispatch management. In the presence of this uncertain request, producers need smart controllers to meet thermal demand and, at the same time, to maximize profit while fulfilling the needs of the grid. This work presents a hierarchical predictive control architecture for optimal management of combined heat and power production sites equipped with a thermal energy storage tank supplying district heating networks. The feasibility of the proposed approach is investigated by simulating several scenarios with different degrees of uncertainty about the actual power request from the grid operator. It is shown that the controlled system is able to comply with the requirements to the maximum extent when the exact power dispatch is known a few hours in advance, also giving a profit increase as well as environmental benefits. While the grid operator request for flexibility is met up to 100%, the reduction in carbon emissions ranges from 3% to 7% and the operating margin is increased by 20%. This can be realized when the power availability is scheduled at periods of both maximum and minimum heat demand. Thus, the method is promising

---

also in improving production planning of future integrated energy systems from the perspective of grid flexibility.

---

1. Introduction

Over the last couple of decades, technological advancements and support policies have fostered the increasing cost-effectiveness of renewable energy compared to conventional fossil fuel-fired power plants. This has led to significant growth in the global market for renewable energy technologies, such as wind, solar and hydropower. For instance, also thanks to these incentives, the renewable power generation capacity in Italy grew by 170% between 2004 and 2018 [1]. Likewise, the primary renewable energy production within the EU-28 increased overall by 64% between 2007 and 2017, which is equivalent to an average growth of 5.1% per year [2]. Such a significant increase in the production of energy from renewable sources has also led to the diffusion of distributed generation, namely power generation performed by a variety of small devices connected to the grid. This spread of distributed generation introduces a significant randomness in the management of the electricity system, since most of the distributed energy resources are renewable energy generators. Furthermore, since grid stability must always be guaranteed by the grid operator, the integration of a large number of discontinuous production units into the existing electricity grid represents an important technical challenge. Aggregating multiple producers or consumers [3] is considered one of the best solutions for addressing these problems, as it allows separate devices to act as a single entity when interacting with the grid operator.

Legislation closely followed the evolution of the electricity system: for instance, Terna, the Italian Transmission System Operator (TSO), recently adopted a specific regulation for a pilot project which

involves the so-called UVAMs (which can be translated as Mixed Aggregated Virtual Units) [4]. These are devices or aggregators connected to the grid that are enabled to provide ancillary services such as congestion resolution, power reserve and grid balancing. In essence, the act regulates the interactions between the TSO and all UVAMs that have previously declared their availability to carry out grid services during a defined time interval. Therefore, each available UVAM must be ready to produce (or consume) a certain amount of power, regardless of whether or not that electricity is eventually requested by the grid operator.

On these grounds, flexibility has become a crucial feature as it allows a power plant to cope with uncertainties of demand [5]. Hence, cogeneration is one of the most suitable and most flexible ways to fulfill the electricity requirements without affecting the overall efficiency of the plant. In fact, a Combined Heat and Power (CHP) plant, if properly designed, can compensate the intermittency of renewable electrical generation, recovering the heat otherwise wasted for heating purposes [6]. This is further specified in a review by Wang et al. [7], in which the authors state that conventional generation units such as CHP plants remain a fundamental value in the energy system in terms of keeping the electricity and heating sectors more reliable and cost-effective. Moreover, CHP plants play an important role in the integration of different energy sectors. Nonetheless, the most profitable exploitation of the technical flexibility of these plants is essential for providing a secure and efficient operation of the integrated energy system [8].

For this reason, research studies on CHP plants and their integration with the power grid have become more widespread [9]. Li et al. [10] formulated a CHP dispatch method to coordinate the operation of electrical power systems and district heating networks (DHNs): they proposed a model which considers the temperature dynamics of the DHN for exploiting energy storage as an option for managing the variability of wind energy. They also demonstrated the potential benefits of this method in terms of operation economics and wind power utilization. Also Xu et al. [11] argue that DHNs are key elements in providing flexibility to the power grid and they give an estimation of this. The

behavior of a DHN is approximated by multiple simple DHNs with a single-producer single-consumer structure.

All these works aim to achieve sector coupling i.e. integration of different energy domains [12] to exploit their synergies and flexibility, especially through bridging district energy and electricity networks. This improves the overall economic performance but also presents many barriers (e.g. control solution complexity), which are thoroughly reviewed by Møller Sneum [13].

In this regard, a smart controller becomes essential since it can regulate the operation of the CHP according to both electrical and thermal requirements, thus trying to avoid partial load operation and consequent efficiency losses. An adequate management strategy for this type of plant should be economically optimal but also robust enough to fulfill the thermal demand of the users connected to the system, at all times, as well as the potential requests from the grid operator. Hence, it has to deal with uncertainty. Based on a review by Zakaria et al. [14], various approaches are available to consider the uncertainty of different elements in the optimization of renewable energies. Monte Carlo simulation is one of the most remarkable methods, and it is used to model uncertainties by generating different scenarios based on the probability of the occurrence of random events. However, the authors conclude that several research questions regarding the dynamics of the integration of renewable energies in the market still remain unanswered. The investigation of multi-scale problems with a high penetration of renewables is an open research field. Skalyga et al. [15] present a robust optimization dispatch model of an integrated electricity and heating system, with wind power uncertainty being modeled by ambiguity sets. In parallel, Gang et al. [16] address uncertainty in the planning and design of district cooling networks, and consider aspects such as outdoor weather, building layout and indoor conditions. Tan et al. [17] propose adaptive robust energy and reserve co-optimization for the integrated electricity and heating system: the goal of minimizing the total cost of the system is achieved by exploiting the additional reserve capacity provided by the district heating system flexibility and by considering the spatial correlation between wind uncertainty. They conclude that

the economic efficiency is improved. Moretti et al. [18] investigate the issues related to generic multi-source energy systems by proposing a robust optimization method for their day-ahead scheduling. However, comprehensive studies on the control of these grids in the context of electricity grid flexibility are not yet available or are at an early stage [19].

Among the new research trends, Model Predictive Control (MPC) methods have been recently studied to improve economic performance [20] or provide grid services. For instance, Vrettos et al. [21] propose a new control framework based on robust MPC for the scheduling and provision of secondary frequency control reserves by means of the heating systems of aggregations of commercial buildings, while Bünning et al. [22] adopt MPC with affine policies to optimally manage heat pumps and perform frequency regulation. In these references, the MPC is applied only to a portion of the system, the aim is frequency control, and the uncertainty on the electrical power request from the TSO, planned according to the market conditions, is not accounted for.

In the light of this, and to the best of the authors' knowledge, there are no literature references regarding the application of MPC to complex energy systems, in order to provide a flexibility service to the power grid (e.g. as UVAM) under demand uncertainty. This paper aims to address this research gap by proposing an MPC control strategy that includes the uncertainty of the TSO power dispatch in the operation of a flexibility provider comprising a CHP plant and a thermal storage unit coupled with the DHN of a small group of end-users. The approach entails a distributed hierarchical control architecture and a two-stage stochastic optimization model with extreme scenarios to account for the uncertainty. It is verified and tested by simulating different cases of interaction with the TSO.

The main novel features of the work, with respect to the existing literature, can be summarized as follows:

- *smart management of a complex energy system* (i.e. comprising a heat distribution network for several buildings and different energy conversion components) as a flexibility provider to the power grid;

- a novel method based on a *multi-level MPC controller* that covers all sections of the energy system;

- stochastic optimization to include the *uncertainty on the actual flexibility request from the TSO* (in terms of electrical power to be produced) within the MPC, which then defines a suitable optimal management strategy to deal with all potential events (e.g. TSO request, absence of TSO request).

The proposed scheme is built in a modular and generic way, thus it is suitable for replication to several flexibility aggregators, with the aim of fostering the transition toward smart energy systems and sector coupling.

2. Methods and control strategy

This section presents the novel method to operate cogeneration plants feeding district energy networks as flexibility providers. The proposed control architecture is based on multi-agent hierarchical Model Predictive Control, and has been demonstrated by the authors in [23]. One simulation case study on the heat distribution network of three education buildings supplied by a biomass-fired Organic Rankine Cycle resulted in a 7% and 12% reduction in operating costs and fuel consumption, respectively, with regard to a traditional controller. In addition, two real-world case studies in operational conditions showed a 13% to 34% reduction in specific energy consumption with regard to the previous management strategy, as well as higher cost-effectiveness [23]. These achievements assessed the superiority of the MPC compared to conventional approaches.

In the present work, the MPC control strategy includes, within the optimization of the power production system coupled with the heat distribution network, the uncertainty deriving from the potential power request from the TSO. This feature aims to enable the controller to provide a flexibility service to the power grid in several conditions. The following sections illustrate the original control architecture and the implementation of the uncertainty. Then, the controller is applied to a simulation case study so that the control performance can be evaluated in different scenarios, which are characterized by different degrees of knowledge of the actual power request.

2.1 Model Predictive Control

Model Predictive Control is a class of control strategies that exploit the prediction of the controlled system behavior over a time horizon in the future (i.e. prediction horizon), carried out through a dynamic model, in order to obtain an open-loop sequence of future control actions that minimize a given cost function (e.g. economic or energy cost). The first input of this sequence, corresponding to the first time-step of the prediction horizon, is applied to control the real system or its simulator, while the remaining inputs are discarded. Afterward, the system states are measured or estimated, the

prediction horizon is shifted one step forward, and an updated optimization problem is created and solved. This procedure, which is carried out continuously, realizes implicit feedback on the actual evolution of the system and reduces the influence of modeling approximations and unpredictable events [24]. Furthermore, *feed-forward* MPC is obtained if the optimization also relies on the prediction of exogenous variables (i.e. disturbances), which is updated at each new time-step. In this way, the controller is able to anticipate the effects of any disturbance, instead of reacting to the occurrence of such disturbance (conventional feedback), and to improve its performance.

The proposed MPC architecture, illustrated in Figure 1 for the case of a school complex, is specifically suitable for small-scale DHNs, in which each building can be considered individually, and achieves optimal management of the distribution network and energy production site. Since the solution of an optimization problem for each simulation time-step is necessary for MPC to be implemented, method feasibility at district level is enabled by splitting the network into its different branches, each feeding one of the buildings and controlled by a dedicated low-level MPC agent, also named building-MPC [25]. This minimizes the heat delivered to the building by varying the heat distribution variables and forecasts the related heat demand for the entire prediction horizon. This information is sent to a high-level MPC agent, namely supervisory-MPC, the duty of which is to operate the cogeneration plant and manage the state of the storage in the energy production site in an optimal way, in order to maximize the operating margin, i.e. the difference between operating revenues and costs. The complete details of the MPC multi-agent modules [26] and supervisory module are given in the following sections.
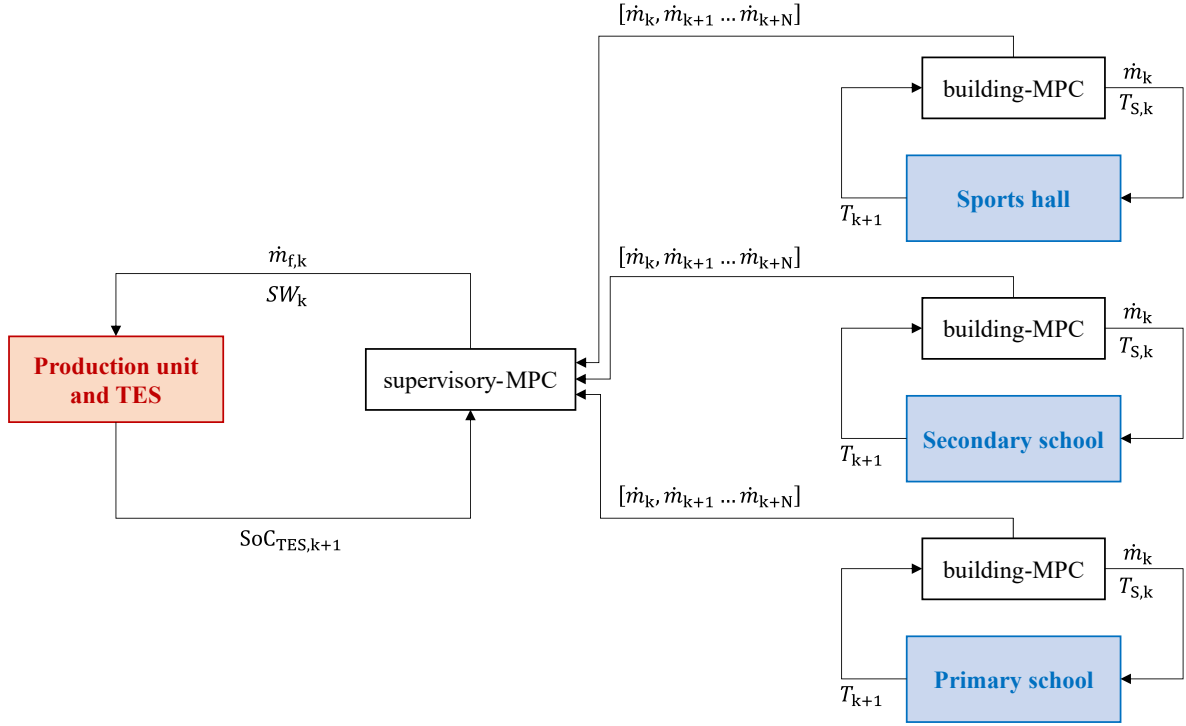
Figure 1. Multi-agent hierarchical architecture of the MPC control strategy for small-scale heating networks.

2.2 Multi-agent modules

The building-MPC has firstly been demonstrated by the authors for the heat distribution network of an individual building, the indoor temperature of which (i.e. T) is the system state [27]. Each building is represented by the discrete form of the energy conservation equation in Eq. (1):

$$\frac{\Delta T}{\Delta t} = -a\,(T - T_{\text{ext}}) + b\,\dot{m}\,c\,(T_S - T_R) \tag{1}$$

with T_{ext} being the ambient temperature and c being the water specific heat capacity. The manipulated variables (i.e. system inputs) are the mass flow rate $\dot{m}$ and the supply temperature T_S of the water to the building substation heat exchanger, while the return temperature T_R is a design parameter regulated by the secondary side as in [25]. The performance coefficients a and b are characteristic of each building and can be identified with real measurements or simulation data [28]. The presented model form with its modularity and little required information provides significant advantages when extending the approach to district energy.

The cost function J_b minimized by each building-MPC for the entire prediction horizon N includes (i) the total supplied heat comprising the heat losses from the pipelines $\dot{Q}_{loss}$; (ii) the pump power P_{pump}, which is a function of the water mass flow rate and pipe features:

$$J_b = \sum_{k=1}^{N} \left[\dot{m}_k\, c \left(T_{S,k} - T_{R,k} \right) + \dot{Q}_{loss,S,k} + \dot{Q}_{loss,S,k} + P_{pump,k} \right] \Delta t + \phi_{b,k} \tag{2}$$

The penalty factor ϕ_b is added when the indoor heating requirements are violated, therefore pushing the solution away from unacceptable conditions. The resulting optimization problem is solved by an original optimization algorithm based on the Dynamic Programming numerical formulation [25]. The algorithm computes the results in a few seconds with a standard computer, thus it is feasible for real-time MPC implementation. At each time-step, the algorithm receives the actual indoor temperature and returns the optimal sequence of water mass flow rate and supply temperature (Figure 1), the first elements of which are implemented as set-points to be kept in the real system.

2.3 Supervisory module

The supervisory-MPC controls the energy production site, hence it requires simplified models of the CHP plant and of the Thermal Energy Storage tank (TES), which is an essential unit for enhancing the flexibility of a system.

The TES is modeled through the thermocline assumption [29,30] presented in Figure 2. This approach is adopted as it provides, as shown in [31], a significant reduction in calculation time while maintaining a good prediction accuracy which are paramount features in MPC applications. The TES is split into two zones, one with the high temperature T_H and one with the low temperature T_L. The height of the virtual separation surface between the zones, with reference to the top of the tank, is defined thermocline and provides an estimation of the State of Energy (SoE) of the TES. The height

of the thermocline X is the system state and its evolution over time depends on the TES characteristics and incoming and outgoing flow rates, according to the following energy balance:

$$\rho A_{\text{TES}} c (T_{\text{H}} - T_{\text{L}}) \frac{\Delta X}{\Delta t} = \dot{Q}_{\text{CHP}} - \dot{m}_{\text{tot}} c (T_{\text{H}} - T_{\text{R}}) - \dot{Q}_{\text{loss,TES}} \tag{3}$$

where ρ and A_{TES} are the water density and tank base surface, respectively, $\dot{Q}_{\text{CHP}}$ is the incoming thermal power, and $\dot{m}_{\text{tot}}$ is the total mass flow rate requested by the end-users downstream and communicated, as a model disturbance, by the building-MPCs. The state X is limited between 0 and the TES total height H_{TES}.
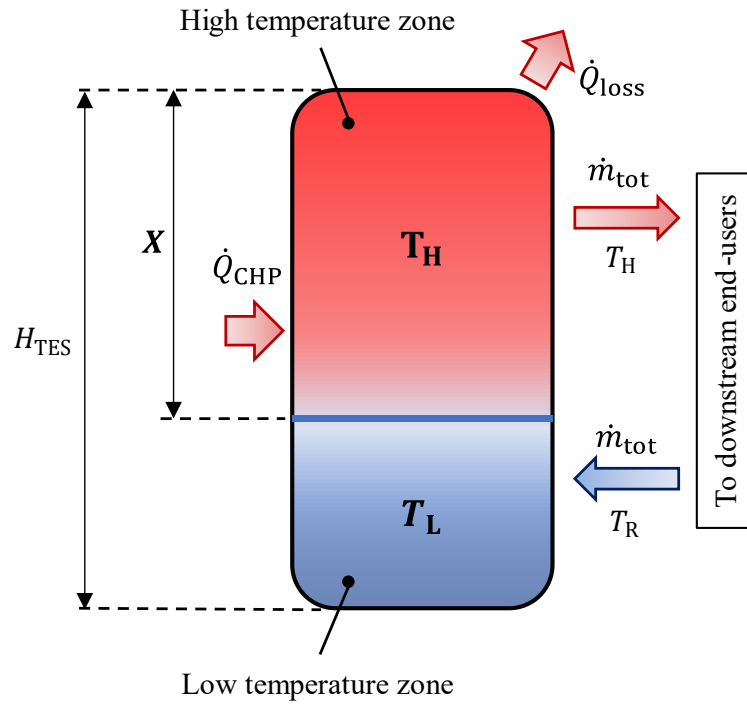

Figure 2. Representation of the Thermal Energy Storage tank with thermocline assumption.

The heat lost to the environment through the TES shell is given by:

$$\dot{Q}_{\text{loss,TES}} = \pi D_{\text{TES}} U_{\text{TES}} [X(T_{\text{H}} - T_{\text{ext}}) + (H_{\text{TES}} - X) (T_{\text{L}} - T_{\text{ext}})] \tag{4}$$

with D_{TES} and U_{TES} being the tank diameter and heat transfer coefficient.

As for the CHP plant, its model is characterized by the first principle efficiency and electrical efficiency, defined by Eqs. (5) and (6), respectively:

$$\eta_I = \frac{P_{CHP} + \dot{Q}_{CHP}}{\dot{m}_f\, LHV} \tag{5}$$

$$\eta_{el} = \frac{P_{CHP}}{\dot{m}_f\, LHV} \tag{6}$$

where $\dot{m}_f$ is the fuel mass flow rate and LHV is its lower heating value. In order to represent the derating of the CHP performance at partial loads, these efficiencies are defined by linear correlations with the load itself, between the minimum and nominal operating conditions of the unit.

Consequently, the thermal power directly supplied to the TES by the CHP and the electrical power produced by the CHP are calculated through Eqs. (7) and (8), respectively:

$$\dot{Q}_{CHP} = \dot{m}_f\, LHV\, (\eta_I - \eta_{el})\, SW \tag{7}$$

$$P_{CHP} = \dot{m}_f\, LHV\, \eta_{el}\, SW \tag{8}$$

Since the CHP is switched off for loads lower than the minimum load conditions, it is necessary to include the on-off signal SW in the model. This is a binary variable equal to 1 or 0 if the plant is operating or not.

The electrical power produced by the CHP in Eq. (8) is exploited to firstly satisfy the electricity demand of the buildings connected to the district heating network P_{dem}, then the exceeding power is exchanged with the grid either to meet the TSO request when applicable, or to sell the surplus. The electrical energy balance Eq. (9) has to be satisfied at all times:

$$P_{CHP} + P_{bg} = P_{sg} + P_{dem} \tag{9}$$

with P_{sg} and P_{bg} being the electricity sold and bought from the grid, respectively.

The system manipulated variables are the fuel mass flow rate, binary on-off signal, and bought electricity. The latter covers the end-users' demand when P_{CHP} is not enough. The objective function

J_s includes the total costs of fuel and electricity purchasing, as well as the revenues from the sale of the electricity:

$$J_s = \sum_{k=1}^{N} \left[\left(C_f \dot{m}_{f,k} + C_{bg} P_{bg,k} - C_{sg} P_{sg,k} \right) \Delta t + \phi_s \right] \tag{10}$$

with C_f, C_{bg} and C_{sg} being the specific costs of the fuel, and bought and sold electrical power, respectively. Similarly to the building-MPC, in order to obtain a feasible solution, the penalty factor ϕ_s is added when the TES state constraints are exceeded and when the TES energy content is not able to comply with the downstream thermal demand.

This problem is solved by a dedicated version of the fast Dynamic Programming algorithm mentioned above. Overall, the supervisory-MPC receives the current SoE of the TES as well as the following disturbances over the prediction horizon: predicted thermal and electrical demands, and the power made available to the TSO. Then, at each time-step, it returns the optimal set-points to operate the CHP in order to guarantee that the TES is able to fulfill such demand.

2.4 Implementation of the TSO request uncertainty

As flexibility provider, the plant operator establishes a reserve of electrical power that is made available to the TSO according to a defined time schedule. In reality, the grid operator, which is responsible for power grid balancing, plans and requests power production from the dispatchable generation plants connected to the grid according to the actual system and market conditions. Hence, the power made available by the plant operator is not actually requested and exploited at all times. The actual request from the TSO is unknown to the plant operator and cannot be easily forecast. For this reason, the supervisory-MPC described in Section 2.3 must be customized to include the uncertainty of the electricity request from the TSO. This is done through a two-stage stochastic

optimization model with extreme scenarios, implemented by considering that, when power availability has been assigned, two events may occur:

- E1: the TSO does not require the available power;

- E2: the TSO requires the entire amount of available power from the generation plant.

In the former case, the objective of each step of the optimization problem is defined by the argument of the sum in Eq. (10), which becomes $J(E1)$. On the contrary, the occurrence of E2 is associated with a modified cost function in which the amount of electricity requested by the TSO and actually dispatched P_{TSO} is rewarded more than in the usual case, i.e. with a specific cost C_{TSO} higher than C_{sg}, since the power plant is providing a service:

$$J(E2) = \left[C_f \dot{m}_f + C_{bg} P_{bg} - C_{sg} (P_{sg} - P_{TSO}) - C_{TSO} P_{TSO} \right] \Delta t + \phi_s \tag{11}$$

According to [32], the expected value of the global cost function of the supervisory-MPC is obtained by weighting the costs of the events E1 and E2 with the related probability of occurrence ω:

$$J_{tot} = \sum_{k=1}^{N} \left[\omega_{1,k} J_k(E1) + \omega_{2,k} J_k(E2) \right] \tag{12}$$

Even though the solution obtained in this way may be suboptimal with respect to the deterministic problem, it allows the most probable events to be effectively considered.

3. Application

The MPC controller with the implementation of uncertainty described in Section 2 is tested in a Model-in-the-Loop (MiL) simulation scenario. A detailed mathematical model, also called system *digital twin*, which reproduces the system dynamics and its interactions with the environment typically faster than real-time, is controlled by a model of the controller, in which the control algorithm code is integrated. This allows the control logic and performance to be verified in analog conditions without affecting the real system. The case study, digital twin configuration and simulated scenarios are described in the following sections.

3.1 Case study description

The case study, represented in Figure 3, is a small-scale district heating network which supplies an education complex consisting of three different buildings: a sports hall, a secondary school and a primary school. An internal combustion gas engine with heat recovery provides electrical and thermal power to the users. The CHP nominal and minimum load conditions as well as the related electrical and first principle efficiencies are reported in Table 1. Depending on CHP operation, TSO request and user demand, the electrical power can be sold or purchased by means of a bidirectional connection with the power grid. The heat recovered by the CHP cannot be dissipated and is entirely supplied to a TES with a total water volume of 200 m^3 (Table 2) in a two inlets-two outlets configuration [33] by means of the main circuit. The TES size was selected according to [34], in which it is stated this unit should be able to fulfill the circuit peak load for 1.5 h to 2 h. Being the thermal peak load equal to 2.5 MW and the design temperature difference between supply and return equal to 20 °C, the chosen water volume fulfills this requirement.

Thus, the TES decouples the production of hot water completely from its distribution, which is directly fed to the buildings by means of three secondary circuits. Once the thermal power has been transferred to the building space heaters, the water is partly recirculated to the building itself to

15

regulate the supply temperature and is partly conveyed to the return manifold, which directly feeds the TES on the user side.
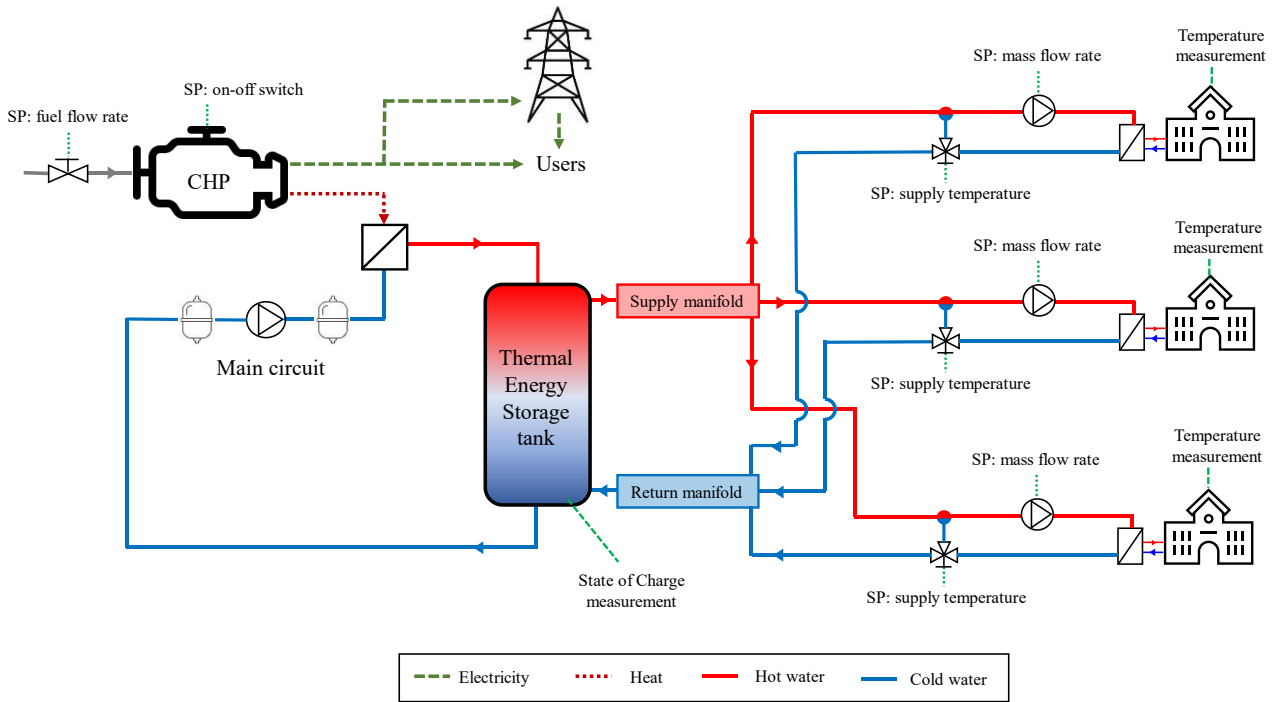

Figure 3. Schematic representation of the case study: small-scale district heating network supplied by a CHP (as flexibility provider) and a storage tank. **SP**: set-point.

Table 1. Main parameters of the Combined Heat and Power plant.

Parameter	Nominal condition	Minimum load condition
Electrical power	2160 kW	220 kW
Electrical efficiency	0.43	0.31
First principle efficiency	0.93	0.84
Fuel LHV	36.6 MJ Nm^{-3}	

Table 2. Main parameters of the Thermal Energy Storage tank and its model.

Parameter	Symbol	Value
Internal diameter	D_{TES}	6.5 m
Height	H_{TES}	6 m

Heat transfer coefficient	U_{TES}	0.25 W m^{-2} K^{-1}
High temperature zone	T_H	80 °C
Low temperature zone	T_L	60 °C

The actual control loops dealing with the system operation management are featured as follows:

- The high-level MPCs establish the set-points according to the solution of the related optimization problem, as explained in Section 2.

- The low-level controllers regulate the actuators in order to track these set-points. In particular, the water mass flow rate to each building is tracked with a feedback loop on the pump rotational speed, while the supply temperature is maintained by setting the recirculation valve with an open-loop controller. In addition, the operation of the building heating elements (e.g. radiators and fan coils) is governed in order to keep the water outlet temperature at the design value of 60 °C.

- When the available power is actually requested from the TSO and the storage is not full, i.e. capable of accepting heat, an auxiliary feedback loop corrects the fuel mass flow rate established by the MPC in order to accurately meet this request. Indeed, when not requested and even if more cost-effective for the system, a higher production may compromise the stability of the power grid.

- Another proportional feedback loop regulates the main circuit pump in order to set the inlet water at the same temperature as the TES high temperature (i.e. 80 °C).

Finally, the cost parameters used in this MiL application are reported in Table 3. The electricity price, considered constant, does not hinder the generality of the approach, since it is possible to include variable prices as predicted disturbances.

Table 3. Specific cost parameters of electricity and fuel in the MiL case study.

Parameter	Symbol	Value
Electricity bought from grid	C_{bg}	160 € MWh^{-1}
Electricity sold to grid	C_{sg}	80 € MWh^{-1}
Electricity fulfilling TSO request	C_{TSO}	400 € MWh^{-1}
Fuel	C_f	0.356 € Nm^{-3}

3.2 System digital twin

The case study simulation is implemented in the MATLAB®/Simulink® environment. The digital twin that emulates the real system is built by means of a library of models of energy system components. These are assembled in a modular way to represent the system configuration of the presented case study. The component blocks adopt a direct causality by considering the flows of matter and energy that enter, exit or are stored within each unit, in order to provide a proper physical representation during transients or in steady state. Each physical element is described by the governing conservation equations in differential or algebraic form and considers both the hydraulic and thermal domains. The library has been presented and used in previous studies [23,27,35] as a reliable tool for accurate simulations of different DHNs.

Particular importance has to be paid to the TES digital twin which, unlike the simplified thermocline model used within the MPC, is based on a one-dimensional, multi-node approach. In this way, it simulates more accurately, but with a higher computational effort, the thermal stratification phenomenon occurring within a sensible heat storage tank, as thoroughly reported in [36]. In this application, the tank is divided into $n = 5$ nodes, each at a temperature T_{node}. Thus, the tank SoE is estimated by the following balance:

$$\text{SoE}_{\text{TES}} = \frac{\frac{\sum_{i=1}^{n} T_{\text{node,i}}}{n} - T_{\text{L}}}{T_{\text{H}} - T_{\text{L}}} \tag{13}$$

3.3 Simulated scenarios

According to a defined schedule, the plant operator makes 1600 kW available to the power grid – as a flexibility service – in a certain period of the day each day. As mentioned in Section 2.4, the available power can be requested by the TSO (E2) or not (E1).

Different scenarios, with reference to the actual knowledge of occurrence of events E1 and E2, are simulated and compared, in order to assess the proposed control strategy with uncertain request from the TSO.

The four considered scenarios are summarized in Table 4 and illustrated in Figure 4 together with the weights ω in the global cost Eq. (12):

- Scenario 0 (S0): baseline scenario in which the supervisory-MPC does not include the potential request of the TSO in the model prediction and optimization. The system reacts to the request at the time it is submitted.

- Scenario 1 (S1): the plant operator knows in advance the exact occurrence of E1 or E2 for the next few hours (e.g. three hours earlier), presumably when the TSO carries out production and dispatch planning. In the rest of the prediction horizon, E1 and E2 are considered equally probable events. The related cost functions appear in the global cost function with a weight equal to 1 for the first three hours and to 0.5 for the rest of the prediction horizon. This scenario is expected to be the most similar to reality.

- Scenario 2 (S2): the plant operator has no exact information regarding the occurrence of E1 or E2. The events are considered equally probable over the entire prediction horizon and, therefore, equally weighted in the global cost function.

19

- Scenario 3 (S3): the plant operator assumes that the power made available is always requested by the TSO and, thus, E2 is always expected when availability is scheduled.

Table 4. Summary of the four simulated scenarios with the weights of the cost functions of E1 and E2 when power availability has been assigned.

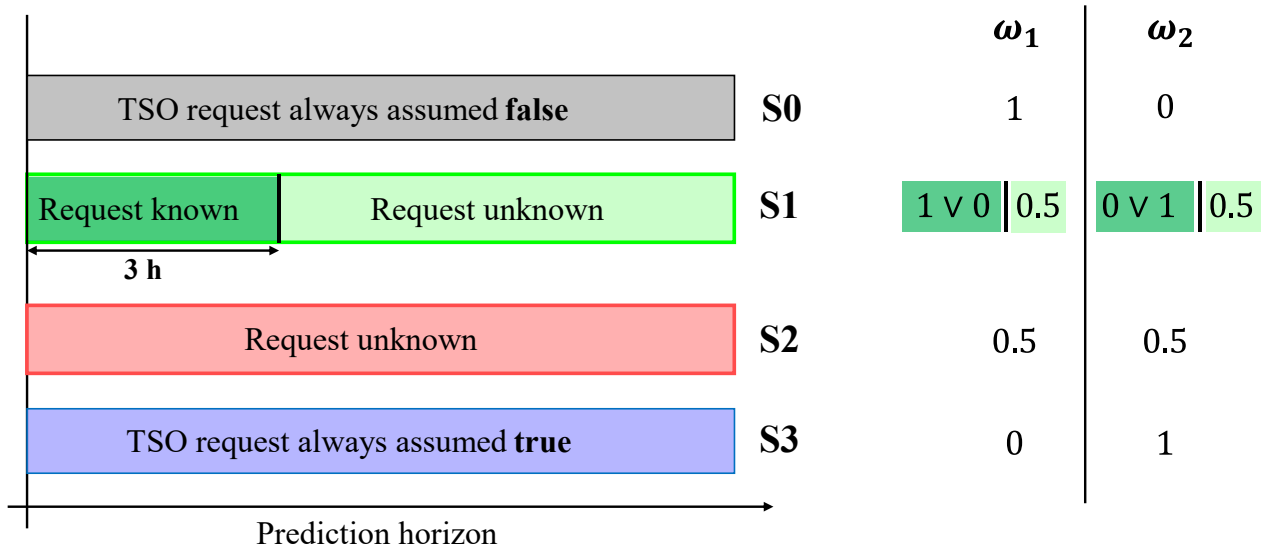| Scenario	Short description	Weight of E1	Weight of E2
S0	Only E1 considered over prediction horizon	1	0
S1	E1 or E2 occurrence known three hours before, and equally probable over rest of horizon	1 ∨ 0 | 0.5	0 ∨ 1 | 0.5
S2	E1 and E2 equally probable over prediction horizon	0.5	0.5
S3	Only E2 considered over prediction horizon	0	1

Figure 4. Schematic representation of the four simulated scenarios with the cost function weights of E1 and E2.

3.4 Key Performance Indicators

In order to evaluate and compare the results of the different scenarios and conditions, six Key Performance Indicators (KPI) have been selected:

- *Operating cost [€]*: the cost of the plant operation, as given by Eq. (14):

$$\text{Operating cost} = C_{\text{bg}}E_{\text{bg}} + C_{\text{f}}m_{\text{f}} \qquad (14)$$

where E_{bg} is the amount of electricity bought from the grid and m_{f} is the mass of fuel purchased.

- *Operating margin [€]*: the revenues due to the electricity sold to the grid, net of the operating cost of the plant.

$$\text{Operating margin} = C_{\text{sg}}E_{\text{sg}} + C_{\text{TSO}}E_{\text{TSO}} - C_{\text{bg}}E_{\text{bg}} - C_{\text{f}}m_{\text{f}} \qquad (15)$$

where E_{TSO} and E_{sg} are the amount of electricity sold to the grid in periods during which the flexibility service is or is not requested, respectively.

- *Electrical requirement compliance [%]*: the percentage of compliance with respect to the total electricity requested by the TSO for the operation of the plant as flexibility provider.

- *Fuel consumption [Nm³]*: the total amount of fuel consumed over the entire time span by the CHP.

- *CO₂ emissions [kg]*: the total amount of CO_2 emitted to operate the services requested which consist of *(i)* fulfilling the thermal and electrical needs of the school complex and *(ii)* providing a flexibility service to the grid. This indicator is the sum of the emissions released by the CHP and those related to the grid for the fulfillment of the rest of the electrical needs. The emission factor for the CHP is assumed that of methane, i.e. equal to 2.16 kg_{CO2}/Nm^3_{CH4} [37]. As for the emissions related to the grid, an emission factor equal to 445.5 kg_{CO2}/MWh [38] is adopted.

- *Average conversion efficiency [%]:* the average first principle efficiency of the CHP. This indicates whether the plant has worked close to or far from the most convenient load conditions and is obtained as the total useful energy with respect to the fuel energy consumed.

4. Results and discussion

The network has been simulated for three representative winter days, in which the users need for heating is typically greater. Firstly, power availability is scheduled when it is expected to have the maximum thermal demand from the downstream buildings (i.e. morning), so that the thermal power, produced in combination with the electrical power, can be either exploited to heat up the buildings or stored in the TES, which has a low SoE due to the high thermal demand.

The novel control method, however, may increase system flexibility and make it suitable to work as a grid service provider also at times of minimum thermal demand, i.e. during the night. The need for flexibility during off-peak periods may become increasingly common in the future due to a more widespread use of electric vehicles, which are typically charged during the night, when production by photovoltaic panels is not available. For these reasons, an additional set of simulations in which the power availability is scheduled out of the expected maximum thermal demand is also shown and its results are evaluated.

4.1 Power availability during the morning

In the first case studied, the plant operator schedules 1600 kW available to the power grid from 7:00 a.m. to noon each day. In this period, the TSO may or may not request this flexibility: Figure 5 shows the available and actual electricity requested, as considered in the simulations.
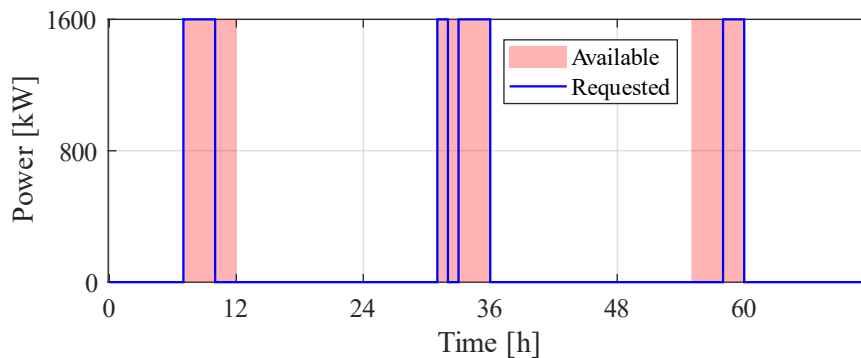

Figure 5. Electrical power made available by the plant operator and actually requested by the grid operator over three representative days (morning case).

The primary goal of the control strategy is to maintain the indoor comfort of the end-users, so it is important to verify the effective delivery of heat. Coherently with previous papers [23,25], Figure 6 shows that the required thermal conditions of the buildings are kept within the limits at all times in all scenarios, confirming the effectiveness of the building-MPCs. Moreover, for each building, it is possible to identify a similar trend in the indoor temperature of the four scenarios. This behavior is reasonable considering that the control strategy of the downstream part of the network is not affected by the management of the generation site, being decoupled from it by means of the TES.
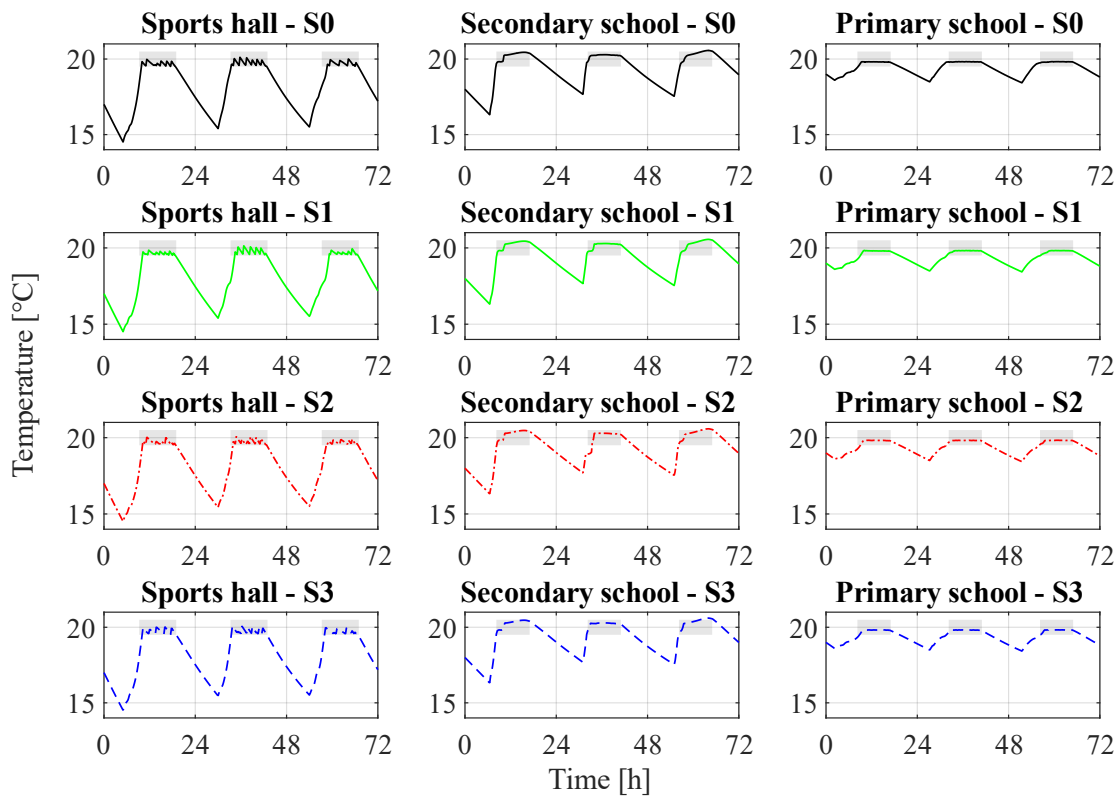

Figure 6. Indoor temperature of the three buildings in the four scenarios (morning case). The shaded area represents the indoor temperature constraints.

Unlike the indoor temperatures, the management of the CHP plant and the TES is different in each scenario since it is influenced by the knowledge of the power requested by the TSO. The power production for each of the four scenarios is represented in Figure 7, and is compared to the actual electricity demand (the shaded area), which is the sum of the electrical needs of the school complex

and the power requested by the TSO. The SoE of the TES, i.e. percentage of energy content of the

water in the tank with reference to the maximum, is represented in Figure 8.
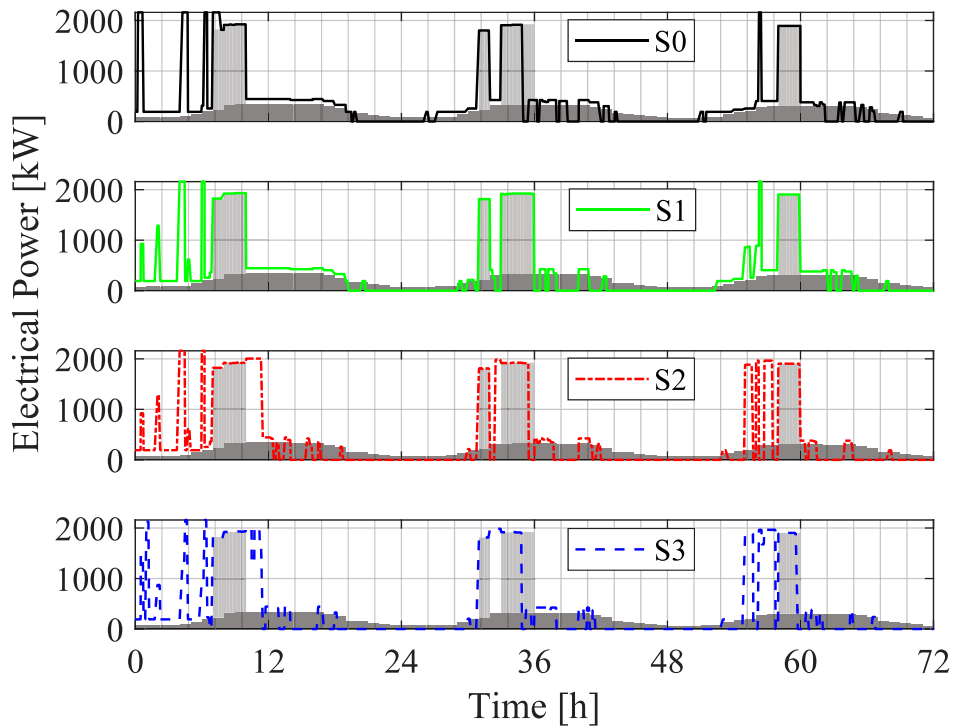

Figure 7. Electrical power produced by the CHP in the four scenarios (morning case). The dark and light shaded areas represent the consumer demand and actual power requested by the grid operator, respectively.
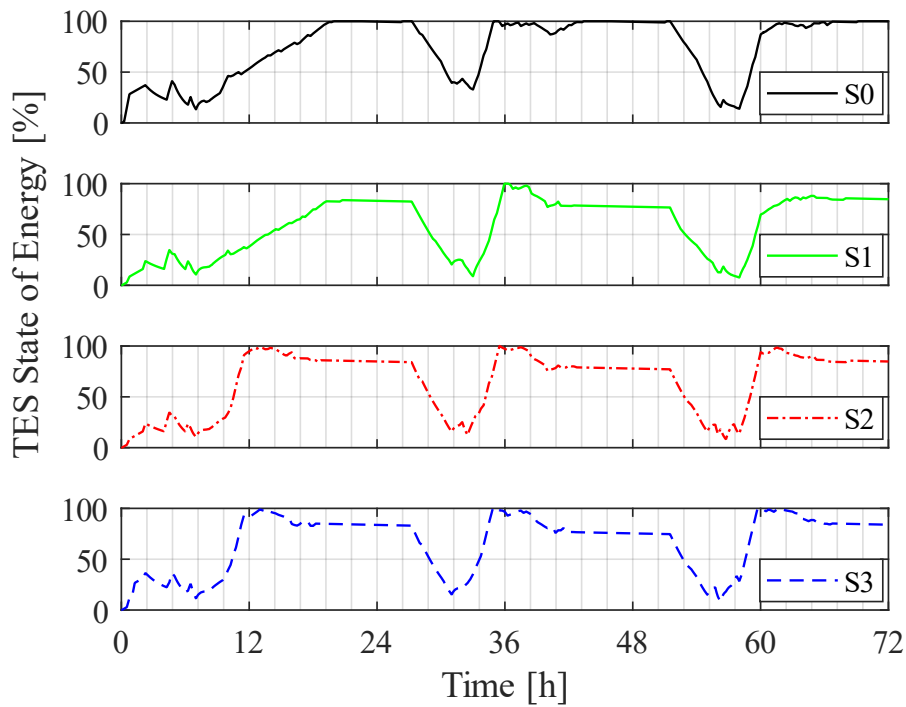

Figure 8. State of Energy of the TES in the four scenarios (morning case).

24

The results show that when the possibility to produce electrical power to provide grid flexibility is considered in the MPC (i.e. S1, S2, S3), the TES is kept emptier in order to leave some margin to store the CHP heat. Indeed, this comes together with the CHP power production which allows the TSO electricity demand to be met. In S0, instead, the request can be met only as soon as it is submitted with the auxiliary feedback loop, and as long as the storage is not full. Since this control is not able to predict the TSO request, the management of the system is not optimal and, in some cases (e.g. in the second day of the simulations), it is not possible for the plant operator to fulfill the total electrical request. In fact, due to the inability to dissipate the extra heat produced by the CHP, the plant switches off when the SoE of the TES reaches the maximum. From Figure 7, it can be observed that S1 gives better results in terms of electrical compliance with the request made by the TSO, since the electricity production follows the demand almost perfectly. In this scenario it is assumed that the TSO request is known exactly three hours in advance, thus the MPC is able to administer the TES with more confidence. As it is the case that better represents reality, S1 presents a promising outcome for real-world implementation.

The total emissions of CO_2 are illustrated in Figure 9, in which the lower part of the bars represents the emissions related to the operation of the CHP plant, while the higher part is the equivalent CO_2 related to the grid in order to meet the portion of the total demand (i.e. both TSO and school complex) not fulfilled by the CHP plant. While the former does not present significant differences in the four scenarios, the emissions related to the grid are considerably lower in S1. This happens because both the TSO request and the user demand are adequately fulfilled in S1, thus the amount of electricity that has to be purchased is lower than in the other scenarios. In S0, electricity from the grid is needed instead to satisfy the TSO request which is not followed by the production of the CHP. Finally, in the scenarios in which there is uncertainty over the entire prediction horizon (S2) and when there is the assumption that the available power is always dispatched (S3), in order to keep a low SoE of the TES as the maximum request from the TSO is expected, the power need of the buildings cannot be fulfilled properly. Consequently, it is necessary to buy electricity to meet the school complex demand. This is

evident from Figure 7, where in S2 and S3 the CHP switches off before the period in which the TSO is expected to request electricity, in order to have enough heat capacity in the TES to meet the demand for the entire availability period. That is reasonable, because the objective of the optimization is the maximization of the operating margin and the reward related to the electricity sold for flexibility purposes is much higher than in other periods.

These results are confirmed by Table 5, in which the KPIs for each scenario are shown. The electrical requirement compliance of S1, in which the constraints of the subsequent three hours are known precisely, is the highest and reaches 99.96%. Indeed, the controller is able to react and operate the system in order to achieve the total power demand. On the other hand, S2 and S3 present a lower electrical compliance: the necessity to produce electricity as a flexibility service is overestimated and, given the limitations on TES capacity, the actual production is planned in less profitable hours. At the same time, in S0, where the potential request of electricity by the grid operator is not considered in the model prediction and optimization, the electrical requirement compliance is equal to 87.19%.

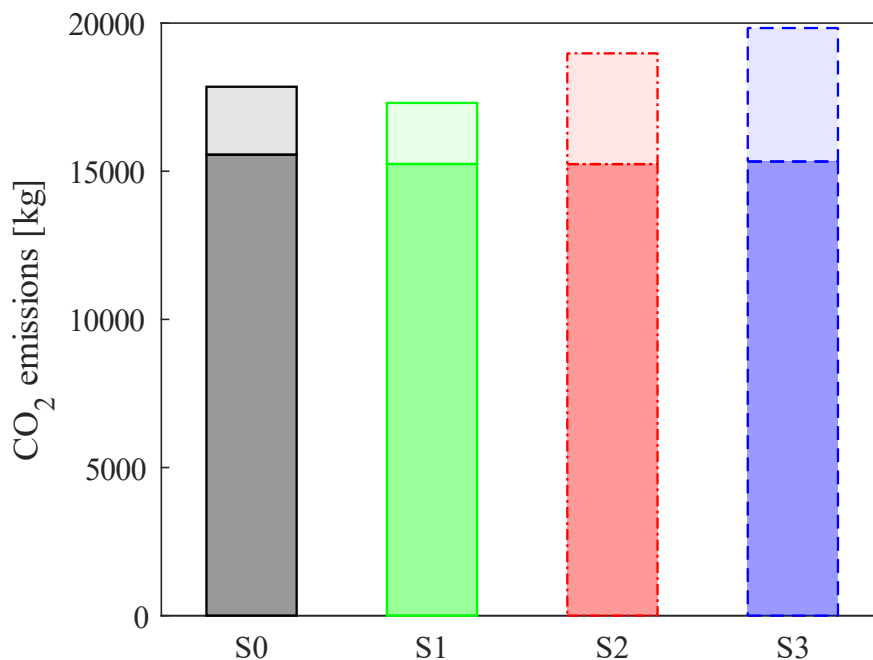Figure 9. Total CO_2 emissions in the four scenarios (morning case) divided into: CO_2 emitted by the CHP plant (lower bars) and by the CO_2 related to the grid in order to comply with the electrical demand of the school complex and of the TSO (higher bars).

Table 5. KPIs in the four scenarios (morning case).

Scenario	Operating cost [€]	Operating margin [€]	Electrical requirement compliance [%]	Fuel consumption [Nm^3]	CO$_2$ emissions [kg]	Average conversion efficiency [%]
S0	3 125	2 434	87.19	7 203	17 850	92.06
S1	3 263	2 941	99.96	7 057	17 310	92.02
S2	3 729	2 409	93.02	7 056	18 980	92.47
S3	3 779	1 896	82.49	7 097	19 830	92.04

It is interesting to note that this parameter is higher in S0 than in S3, in which the TSO request is significantly overestimated. This leads to an inappropriate filling of the TES, which cannot receive the heat that would be produced when fulfilling the actual power request. As for the plant operation, the average conversion efficiency is slightly lower than the nominal first principle efficiency, since the CHP works at lower rates when the TES is not full and only the user demand needs to be met.

Table 6 reports the results in terms of energy production and demand for the four simulations. It can be seen that the total amount of electricity produced by the CHP plant is similar for the four scenarios, though S1 presents the lowest production. In the two scenarios in which it is known that the flexibility service has to be performed, but there is uncertainty about its actual demand, namely S2 and S3, the electricity sold to the grid during times in which it is not requested is more than 30% of the total production, while in S0 and S1 this value is lower (around 20%).

Conversely, S1 has the highest percentage of electricity sold to the grid as a flexibility service (48.1%), being the scenario that better complies with the actual TSO request. The scenario with the highest share of self-consumed energy is S0, followed by S1. This confirms the effectiveness of the control strategy of S0, in which only user demand is privileged, while the TSO request is omitted.

Table 6. Energy results of the four simulations (morning case).

		S0	S1	S2	S3
		[kWh]			
TSO request		14 400			
Production **(share)**	**Total**	**30 397**	**29 924**	**30 171**	**30 233**
	Self-consumed	11 132 **(36.6%)**	9 946 **(33.2%)**	7 028 **(23.3%)**	6 810 **(22.5%)**
	Sold	6 710 **(22.1%)**	5 585 **(18.7%)**	9 748 **(32.3%)**	11 545 **(38.2%)**
	Flexibility service	12 555 **(41.3%)**	14 394 **(48.1%)**	13 395 **(44.4%)**	11 878 **(39.3%)**
Demand **(share)**	**Total**	**14 642**			
	Self-produced	11 132 **(76.0%)**	9 946 **(67.9%)**	7 028 **(48.0%)**	6 810 **(46.5%)**
	Bought	3 510 **(24.0%)**	4 696 **(32.1%)**	7 614 **(52.0%)**	7 832 **(53.5%)**

As for user electrical energy demand, S0 and S1 self-produce 76.0% and 67.9%, respectively, while S2 and S3 do not reach 50%. This happens because in S2 and S3 the plant operator renounces the fulfillment of the electrical needs of the school complex in order to keep the TES empty enough to produce electricity afterward in order to comply with the theoretical TSO request.

4.2 Power availability during the night

In the second case studied, the plant operator schedules the available power during the night, at the time of minimum thermal demand. In order to calculate the maximum time period for which it is possible to entirely satisfy the electrical TSO request in the absence of thermal demand, the total amount of heat that can be stored in the TES is evaluated as follows:

$$Q_{\text{TES}} = m_{\text{H}_2\text{O}}c(T_{\text{H}} - T_{\text{L}}) \tag{16}$$

with m_{H2O} being the water mass contained within the TES, and T_{H} and T_{L} being the high and low temperatures of the tank, according to the thermocline assumption (Section 2.3). Knowing that the power scheduled as a flexibility service is $P_{\text{el}} = 1600$ kW, the corresponding thermal output from the CHP can be calculated as:

$$\dot{Q}_{\text{CHP}} = \frac{P_{\text{el}}}{\eta_{\text{el}}}(\eta_{\text{I}} - \eta_{\text{el}}) \tag{17}$$

Therefore, the time span for which it is possible to fulfill the electrical demand, obtained by means of Eq. (18), is equal to $t = 2.4$ h.

$$t = \frac{Q_{\text{TES}}}{\dot{Q}_{\text{CHP}}} \tag{18}$$

Consequently, in order to guarantee the possibility to fully comply with the TSO request, a period of 2 h of availability is chosen and scheduled from 2:00 a.m. to 4:00 a.m., as shown in Figure 10.
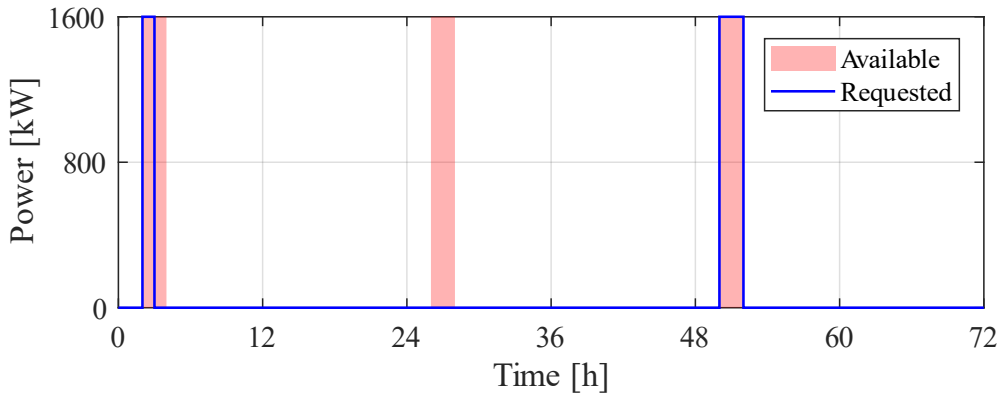

Figure 10. Electrical power made available by the plant operator and actually requested by the grid operator over three representative days (night case).

Coherently with the morning case, the effectiveness of the control strategy in maintaining the end-users' indoor comfort is verified, showing results similar to those exposed in Figure 6.

In Figure 11, the electrical production is compared to the total request (shaded area), which is the sum of the electrical needs of the buildings and the actual flexibility requested by the TSO. The results show that, in the scenarios in which it is expected that the TSO may request a flexibility service (i.e. S1, S2 and S3), 100% electrical compliance is achieved. This is reasonable considering that the total amount of electricity demanded as a flexibility service can, theoretically, be fully met by the plant, using less than the total TES capacity. Nevertheless, it is worth noting that in S1 the production of electricity for flexibility closely meets the request, while in S2 and S3 it pursues the theoretical request of 2 hours in each of the three days, injecting energy surplus into the grid even when not requested. On the other hand, when the control strategy is not aware of the future TSO request (i.e. S0) the results demonstrate that the CHP is not able to fulfill this completely because the TES is not kept empty enough before the request. Indeed, from Figure 12 it is possible to observe that, especially during the third day, when flexibility is requested, the SoE of the TES is already high and it suddenly reaches its maximum, making it unfeasible to satisfy the TSO request, as the additional heat cannot be dissipated.

On the contrary, looking at Figure 12 it is worth remarking that in S1, S2 and S3 the SoE is kept very low during the night, so it is possible to produce all the electricity requested by the TSO. Additionally, in the scenario in which the exact TSO request is known three hours in advance (S1), the CHP does not work during the night if the flexibility is not requested. Indeed, it switches on only when the heat is effectively demanded by the school complex, thus avoiding heat losses to the environment through the TES shell. This behavior also leads to a lower total fuel consumption in S1 compared to the other scenarios (Table 7). With respect to this, it can also be observed that the utilization of the CHP in S0 is characterized by lower steps when the TSO requests flexibility, compared to the other scenarios. This is again coherent with the aim and cost function of S0. As for the comparison of the total CO_2 emissions in the four scenarios, similar considerations to those made for Figure 9 can also be deducted by Figure 13. In particular, S1 is the case with the lowest emissions.
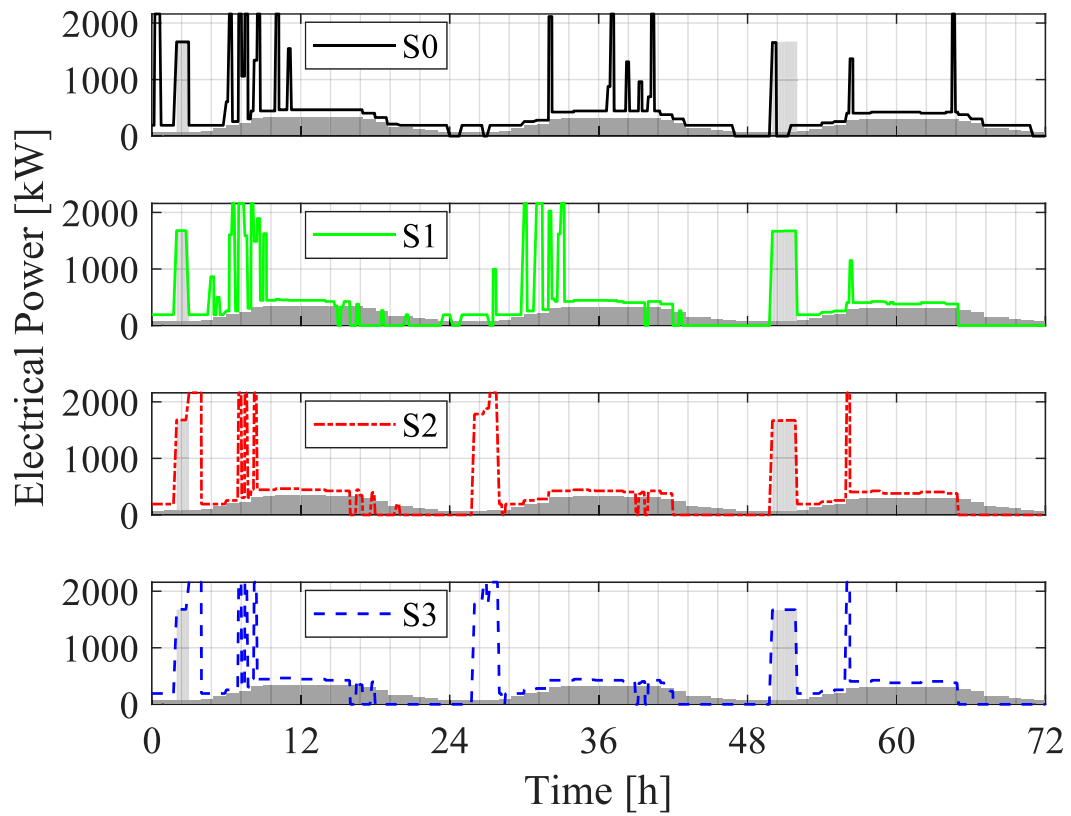
Figure 11. Electrical power produced by the CHP in the four scenarios (night case). The dark and light shaded areas represent the consumer demand and actual power requested by the grid operator, respectively.
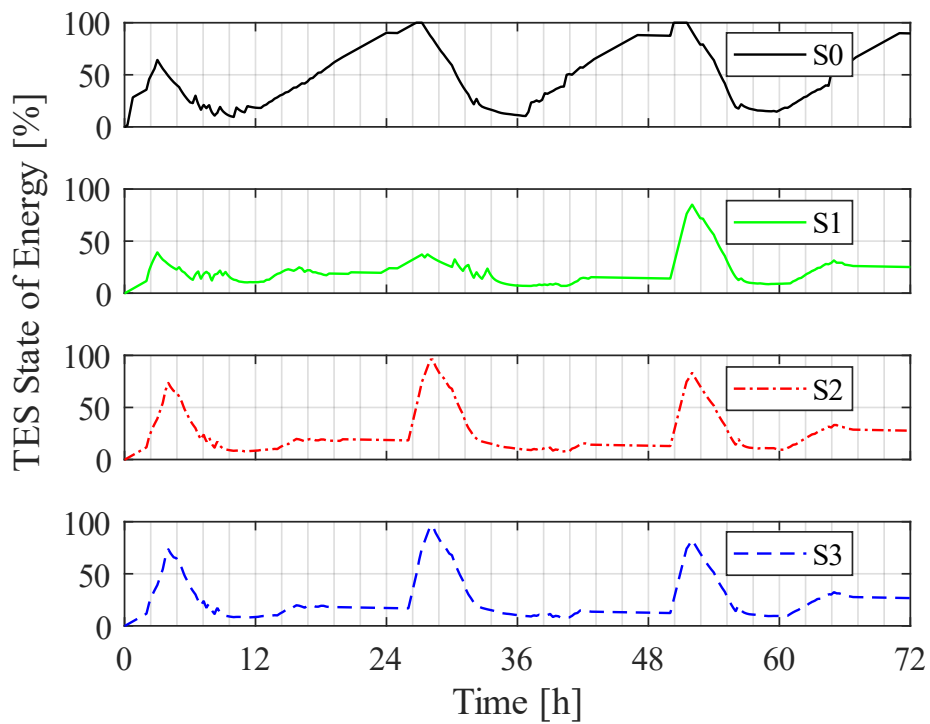

Figure 12. State of Energy of the TES in the four scenarios (night case).

31

Table 7 displays the KPIs obtained in the night case. As already noticed, all the scenarios achieve 100% electrical requirement compliance except for S0, which instead presents the lowest operating margin and the highest fuel consumption and CO_2 emissions. These results confirm that the MPC control strategy used for S1, S2 and S3 effectively increases system flexibility and makes it suitable to work as a power provider also when there is minimum thermal demand. Furthermore, the CHP generally works at a higher load and, thus, conversion efficiency compared to S0, since a higher request is included in the optimization.
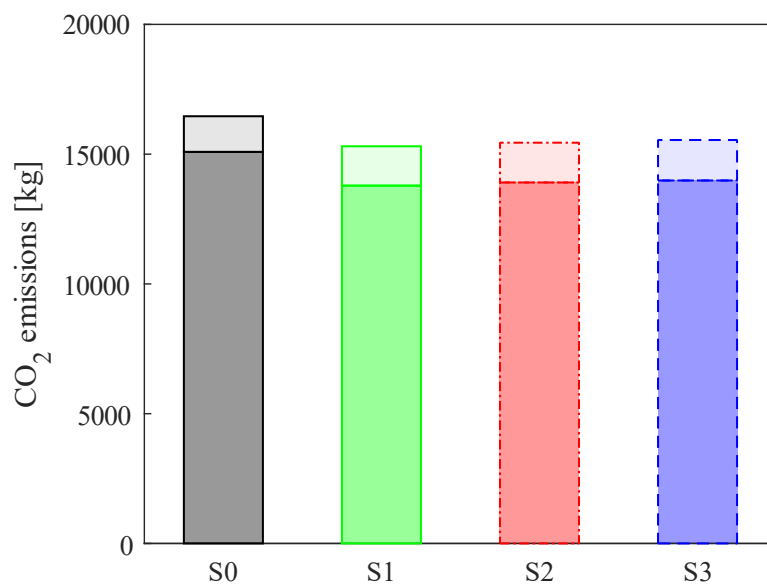

Figure 13. Total CO_2 emissions in the four scenarios (night case) divided into: CO_2 emitted by the CHP plant (lower bars) and by the CO_2 related to the grid in order to comply with the electrical demand of the school complex and of the TSO (higher bars).

Table 7. KPIs in the four scenarios (night case).

Scenario	Operating cost [€]	Operating margin [€]	Electrical requirement compliance [%]	Fuel consumption [Nm3]	CO_2 emissions [kg]	Average conversion efficiency [%]
S0	2 558	- 695	43.86	6 984	16 460	92.01
S1	2 822	- 23.5	100.00	6 383	15 300	92.34
S2	2 856	- 17.5	100.00	6 439	15 440	92.59
S3	2 877	- 36.4	100.00	6 474	15 550	91.99

Looking at Table 8, it can be seen that the total electrical production in S1, S2 and S3 is almost equal, while the production of S0 is higher, and the most part is used for self-consumption. During the availability period, S0 is the scenario which sells less electricity, both in absolute value and in percentage (only 7.2% of the electricity produced is sold as a flexibility service), while this quantity is more than doubled in the other scenarios.

Moreover, S0 fulfills the school complex electrical energy demand up to 96.9% with self-production, buying only 3.1% from the grid, while this purchase from the grid rises up to more than 20% in other scenarios. This is a consequence of the effectiveness of S0 in considering only the user needs and the fact that the other cases put the more remunerative TSO request first.

Table 8. Energy results of the four simulations (night case).

		S0	S1	S2	S3
		[kWh]			
TSO request		4 800			
Production **(share)**	**Total**	**29 063**	**27 123**	**27 431**	**27 439**
	Self-consumed	14 187 (**48.8%**)	11 198 (**41.5%**)	11 114 (**40.6%**)	11 062 (**40.4%**)
	Sold	12 771 (**43.9%**)	10 988 (**40.7%**)	11 481 (**41.9%**)	11 507 (**42.0%**)
	Flexibility service	2 105 (**7.2%**)	4 800 (**17.8%**)	4 800 (**17.5%**)	4 800 (**17.5%**)
Demand **(share)**	**Total**	**14 642**			
	Self-produced	14 187 (**96.9%**)	11 198 (**76.5%**)	11 114 (**75.9%**)	11 062 (**75.5%**)
	Bought	455 (**3.1%**)	3 444 (**23.5%**)	3 528 (**24.1%**)	3 580 (**24.5%**)

4.3 Final remarks

Overall, in both cases (when power availability is scheduled at maximum and minimum thermal demand), the effectiveness of the control strategy based on MPC is verified and regarded as promising, in particular as far as real-world conditions are concerned.

The profit is significant due to the high remuneration of the flexibility service. In the morning case, power availability is scheduled for 5 hours each day and the three-day TSO request amounts to a total of 9 hours. Hence, the resulting operating margin is positive. On the other hand, the night case presents a final TSO request of 3 hours and, consequently, a lower income. Another difference between the two cases can be seen in the average TES SoE, which is much lower when power availability is scheduled during the night, as the total power demand that has to be met is lower.

In addition, this method can be helpful for providing insights in terms of operation and management and, therefore, for discussing and revising production scheduling and design choices.

In light of these results, some improvements can be proposed for further studies:

- The auxiliary controller could be modified in order to avoid electricity production when the flexibility service is not actually requested. Indeed, a large injection of power into the grid, when not requested, may compromise the grid stability, leading to potential harm.

- Another degree of freedom could be added to the current system with the possibility of dissipating the surplus heat produced by the CHP. This would allow thermal and electrical production to act independently.

- Different methods to consider the uncertainty, as well as additional sources of uncertainty (e.g. variability of the external environment conditions or of the electricity market prices), could be investigated to generate a robust MPC.

5. Conclusions

In the current global energy system, there is a growing need for dispatchable electricity generators that can make electrical power available to the power grid operator when requested, in order to deal with the discontinuity of renewable generators. This work proposed a novel method for enhancing grid flexibility by means of the smart control of cogeneration plants coupled with district heating systems and thermal energy storage, which provide the aforementioned service when there is demand uncertainty. Indeed, at selected time intervals, the plant scheduled power availability, which could actually be dispatched or not by the grid operator. The control approach was based on a multi-agent hierarchical Model Predictive Control architecture which minimized building heat consumption and managed the plant and storage to maximize the operating margin while attempting to comply with the electricity request. In order to consider the uncertainty of this parameter, a case study was simulated in several scenarios, in which the actual request of the grid operator was either known, to various extents, or not at all. The control results showed that, while thermal comfort was always guaranteed, the fulfillment of power request was assured to different degrees depending on the scenario. The best performance in terms of compliance with the request (almost 100%), cost-effectiveness and reduction in carbon emissions was obtained in the close-to-reality case in which the power request is precisely known three hours in advance.

Furthermore, the control strategy allowed the flexibility service to be scheduled and provided not only when there was a peak in heat demand (i.e. during the morning) but also when there was low demand (i.e. night hours). Therefore, it has been demonstrated that the proposed predictive controller is a suitable approach for facing the flexibility challenges of future renewable energy systems.

Acknowledgements

References

[1] Gestore Servizi Energetici. Rapporto statistico 2018: Fonti rinnovabili – Available (in Italian) at: https://tinyurl.com/GSEReport [accessed 22.02.2022]

[2] Eurostat – Statistics explained. Renewable energy statistics – Available at: https://tinyurl.com/Eurostat-StatisticsExplained [accessed 22.02.2022]

[3] Yi Z, Xu Y, Wu C. Improving operational flexibility of combined heat and power system through numerous thermal controllable residents aggregation. International Journal of Electrical Power & Energy Systems 2021;130:106841. https://doi.org/10.1016/j.ijepes.2021.106841

[4] Terna. Regolamento recante le modalità per la creazione, qualificazione e gestione di unità virtuali abilitate miste (UVAM) al mercato dei servizi di dispacciamento. – Available (in Italian) at: https://download.terna.it/terna/0000/1071/84.PDF [accessed 22.02.2022]

[5] Heggarty T, Bourmaud JY, Girard R, Kariniotakis G. Quantifying power system flexibility provision. Applied Energy 2020;279:115852. https://doi.org/10.1016/j.apenergy.2020.115852

[6] Jimenez-Navarro JP, Kavvadias K, Filippidou F, Pavičević M, Quoilin S. Coupling the heating and power sectors: The role of centralised combined heat and power plants and district heat in a European decarbonised power system. Applied Energy 2020;270:115134. https://doi.org/10.1016/j.apenergy.2020.115134

[7] Wang J, You S, Zong Y, Træholt C, Dong Z. Y, Zhou Y. Flexibility of combined heat and power plants: A review of technologies and operation strategies. Applied Energy 2019;252:113445. https://doi.org/10.1016/j.apenergy.2019.113445

[8] Ivanova P, Sauhats A, Linkevics O. District Heating Technologies: Is it Chance for CHP Plants in Variable and Competitive Operation Conditions? IEEE Transactions On Industry Applications 2019;55: 35–42. https://doi.org/10.1109/TIA.2018.2866475

[9] Wang W, Jing S, Sun Y, Liu J, Niu Y, Zeng D, Cui C. Combined heat and power control considering thermal inertia of district heating network for flexible electric power regulation. Energy 2019;169: 988–999. https://doi.org/10.1016/j.energy.2018.12.085

[10] Li Z, Wu W, Shahidehpour M, Wang J, Zhang B. Combined heat and power dispatch considering pipeline energy storage of district heating network. IEEE Transactions on Sustainable Energy 2016;7.1:12–22. https://doi.org/10.1109/TSTE.2015.2467383

[11] Xu X, Lyu Q, Qadrdan M, Wu J. Quantification of flexibility of a district heating system for the power grid. IEEE Transactions on Sustainable Energy 2020;11.4:2617–2630. https://doi.org/10.1109/TSTE.2020.2968507

[12] Felten B. An integrated model of coupled heat and power sectors for large-scale energy system analyses. Applied Energy 2020;266:114521. https://doi.org/10.1016/j.apenergy.2020.114521

[13] Møller Sneum D. Barriers to flexibility in the district energy-electricity system interface – A taxonomy. Renewable and Sustainable Energy Reviews 2021;145:111007. https://doi.org/10.1016/j.rser.2021.111007

[14] Zakaria A, Ismail FB, Hossain Lipu MS, Hannan MA. Uncertainty models for stochastic optimization in renewable energy applications. Renewable Energy 2020;145:1543–71. https://doi.org/10.1016/j.renene.2019.07.081

[15] Skalyga M, Wu Q, Zhang M. Uncertainty-fully-aware coordinated dispatch of integrated electricity and heat system. Energy 2021;224:120182. https://doi.org/10.1016/j.energy.2021.120182

[16] Gang W, Augenbroe G, Wang S, Fan C, Xiao F. An uncertainty-based design optimization method for district cooling systems. Energy 2016;102:516–27. https://doi.org/10.1016/j.energy.2016.02.107

[17] Tan J, Wu Q, Hu Q, Wei W, Liu F. Adaptive robust energy and reserve co-optimization of integrated electricity and heating system considering wind uncertainty. Applied Energy 2020;260:114230. https://doi.org/10.1016/j.apenergy.2019.114230

[18] Moretti L, Martelli E, Manzolini G. An efficient robust optimization model for the unit commitment and dispatch of multi-energy systems and microgrids. Applied Energy 2020;261:113859. https://doi.org/10.1016/j.apenergy.2019.113859

[19] Fu DZ, Zheng ZY, Gui J, Xiao R, Huang GH, Li YP. Development of a fuel management model for a multi-source district heating system under multi-uncertainty and multi-dimensional constraints. Energy Conversion and Management 2017;153:243–56. https://doi.org/10.1016/j.enconman.2017.10.002

[20] Lv C, Yu H, Li P, Wang C, Xu X, Li S, Wu J. Model predictive control based robust scheduling of community integrated energy system with operational flexibility. Applied Energy 2019;243:250–265. https://doi.org/10.1016/j.apenergy.2019.03.205

[21] Vrettos E, Oldewurtel F, Andersson G. Robust energy-constrained frequency reserves from aggregations of commercial buildings. IEEE Transactions on Power Systems 2016; 31.6: 4272–4285. https://doi.org/10.1109/TPWRS.2015.2511541

[22] Bünning F, Warrington J, Heer P, Smith RS, Lygeros J. Frequency regulation with heat pumps using robust MPC with affine policies. IFAC-PapersOnLine 2020;53:13210–13215. https://doi.org/10.1016/j.ifacol.2020.12.147

[23] De Lorenzi A, Gambarotta A, Morini M, Rossi M, Saletti C. Setup and testing of smart controllers for small-scale district heating networks: An integrated framework. Energy 2020;205:118054. https://doi.org/10.1016/j.energy.2020.118054

[24] Serale G,Fiorentini M, Capozzoli A, Bernardini D, Bemporad A. Model Predictive Control (MPC) for Enhancing Building and HVAC System Energy Efficiency: Problem Formulation, Applications and Opportunities. Energies 2018;11(3), 631. https://doi.org/10.3390/en11030631

[25] Saletti C, Gambarotta A, Morini M. Development, analysis and application of a predictive controller to a small-scale district heating system. Applied Thermal Engineering 2020;165, 114558. https://doi.org/10.1016/j.applthermaleng.2019.114558

[26] Wernstedt F. Multi-Agent Systems for Distributed Control of District Heating Systems. PhD thesis, 2005. Karlskrona, Sweden: Blekinge Institute of Technology. Available at: http://citeseerx.ist.psu.edu/viewdoc/download?doi=10.1.1.132.7329&rep=rep1&type=pdf [accessed 22.06.2021]

[27] Cadau N, De Lorenzi A, Gambarotta A, Morini M, Saletti C. A Model-in-the-Loop application of a Predictive Controller to a District Heating system. Energy Procedia 2018;148:352–59. https://doi.org/10.1016/j.egypro.2018.08.088

[28] Gambarotta A, Morini M, Saletti C. Development of a model-based Predictive Controller for a heat distribution network. Energy Procedia 2019;158:2896–901. https://doi.org/10.1016/j.egypro.2019.01.944

[29] Campos Celador A, Odriozola M, Sala JM. Implications of the modelling of stratified hot water storage tanks in the simulation of CHP plants. Energy Conversion and Management 2011;52:3018–26. https://doi.org/10.1016/j.enconman.2011.04.015

[30] Dainese C, Faè M, Gambarotta A, Morini M, Premoli M, Randazzo G, Rossi M, Rovati M, Saletti C. Development and application of a Predictive Controller to a mini district heating network

fed by a biomass boiler. Energy Procedia 2019;159:48–53.

https://doi.org/10.1016/j.egypro.2018.12.016

[31] Dickes R, Desideri A, Lemort V, Quoilin S. Model reduction for simulating the dynamic behavior of parabolic troughs and a thermocline energy storage in a micro-solar power unit. Proceedings of the ECOS Conference 2015, Pau, France, 29 June–3 July 2015.

[321] Uusitalo L, Lehikoinen A, Helle I, Myrberg K. An overview of methods to evaluate uncertainty of deterministic models in decision support. Environmental Modelling & Software 2015;63:24-31. https://doi.org/10.1016/j.envsoft.2014.09.017

[33] González-Pino I, Pérez-Iribarren E, Campos-Celador A, Terés-Zubiaga J. Analysis of the integration of micro-cogeneration units in space heating and domestic hot water plants. Energy 2020;200,117584. https://doi.org/10.1016/j.energy.2020.117584

[34] Barbieri ES, Melino F, Morini M. Influence of the thermal energy storage on the profitability of micro-CHP systems for residential building applications. Applied Energy 2012;97:714-22. https://doi.org/10.1016/j.apenergy.2012.01.001

[35] Ancona MA, Branchini L, De Lorenzi A, De Pascale A, Gambarotta A, Melino F, Morini M. Application of different modeling approaches to a district heating network. AIP Conference Proceedings 2019; 2191, 020009. https://doi.org/10.1063/1.5138742

[36] Cadau N, De Lorenzi A, Gambarotta A, Morini M, Rossi M. Development and Analysis of a Multi-Node Dynamic Model for the Simulation of Stratified Thermal Energy Storage. Energies 2019; 12(22), 4275. https://doi.org/10.3390/en12224275

[37] Oficina Catalana del Canvi Climàtic. Practical Guide For Calculating Greenhouse Gas (GHG) Emissions. Version 1 March 2019 – Available at: https://tinyurl.com/CanviClimaticGHGemissions [accessed 22.02.2022]

[38] Istituto Superiore per la Protezione e la Ricerca Ambientale (ISPRA). Fattori di emissione atmosferica di gas a effetto serra nel settore elettrico nazionale e nei principali Paesi Europei. 303/2019. 12 Marzo 2019 – Available (in Italian) at: https://tinyurl.com/ReportISPRA [accessed 22.02.2022]

Nomenclature

A_{TES}	base surface of the storage tank [m^2]
a	first building performance coefficient [s^{-1}]
b	second building performance coefficient [°C kJ^{-1}]
C	specific cost [€/MWh] or [€/kg]
c	water specific heat capacity [kJ kg^{-1} °C^{-1}]
D_{TES}	diameter of the storage tank [m]
E	electrical energy [kJ]
H_{TES}	height of the storage tank [m]
J	cost function [€]
LHV	fuel lower heating value [kJ kg^{-1}]
m	mass [kg]
$\dot{m}$	mass flow rate [kg s^{-1}]
N	number of time-steps [-]
n	number of nodes of the storage detailed model [-]
P	electrical power [kW]
$\dot{Q}$	thermal power [kW]
Q	heat [kJ]
SW	on-off switch [-]
T	temperature [°C]
t	time [s]

U_{TES} heat transfer coefficient of the storage tank [kW m^{-2} K^{-1}]

X height of the thermocline [m]

ϕ penalty for state constraint violation [€]

η efficiency [-]

ρ water density [kg m^{-3}]

ω weight of the event cost in the total cost function

Subscripts

b   building

bg   bought from the power grid

dem   demand

el   electrical

ext   outdoor

f   fuel

H   high temperature zone

I   first principle

k   time-step index

L   low temperature zone

R   return

S   supply

s   supervisory

| sg | sold to the power grid |
| tot | total |

Acronyms

CHP	Combined Heat and Power
DHN	District Heating Network
KPI	Key Performance Indicator
MiL	Model-in-the-Loop
MPC	Model Predictive Control
SoE	State of Energy
SP	set-point
TES	Thermal Energy Storage tank
TSO	Transmission System Operator
UVAM	Mixed Aggregated Virtual Units